

Supporting Information

Smart candle soot coated membranes for on-demand free oil/water mixture and emulsion switchable separation

Jian Li^{*,a,b}, Zhihong Zhao^{‡,a}, Dianming Li^{‡,a}, Haifeng Tian^a, Fei Zha^a, Hua Feng^a, Lin Guo^{*,b}

^a College of Chemistry and Chemical Engineering, Northwest Normal University, Lanzhou 730070, China.
E-mail: jianli83@126.com, Tel: +86 931 7971533.

^b Key Laboratory of Bio-Inspired Smart Interfacial Science and Technology of Ministry of Education, School of Chemistry, BeiHang University, Beijing 100191, P. R. China. E-mail: guolin@buaa.edu.cn

[‡] These authors contributed equally.

CONTENT

1. Materials.....	1
2. Collection of candle soot.....	1
3. Preparation of CSM and CSP.....	2
4. Wettability of CSM.....	2
5. Dynamic adhesion measurements	2
6. The wettability of the original stainless steel mesh	3
7. Oil/water separation of the original stainless steel mesh	3
8. The measurement of environmental stability	3
9. The mechanical strength and abrasion resistance of the CMS	4
10. The stability test of the CSP membrane	5
11. The wettability of the original PVDF	5
12. Water-in-oil and oil-in-water emulsions separation	5
13. Stability tests of the emulsions and separation result of different membrane.....	6
14. Optical microscope images and photographs of the demulsification and separation results for various types of oil-in-water emulsions.....	6
15. Optical microscope images and photographs of the demulsification and separation results for various types of water-in-oil emulsions.....	7
16. Droplet size measurements of different stabilized emulsions for various types of emulsions	8
17. Droplet size measurements of different filtrate after separation for various types of emulsions	9
18. Reference	9

1. Materials

Rapeseed oil and candle were purchased from local store. Oils (hexane, kerosene and petroleum ether) and organic solvents (chloroform, absolute ethanol, toluene, tetrachloroethane and acetone) were purchased from Guangdong Guanghua Sci-Tech Co., Ltd. Sodium alginate (SA), HCl, NaOH and NaCl were purchased from Shanghai Zhongqin Chemical Reagent Co., Ltd. Tween 80 and Span 80 were purchased from Sinopharm Chemical Reagent Co., Ltd.

2. Collection of candle soot

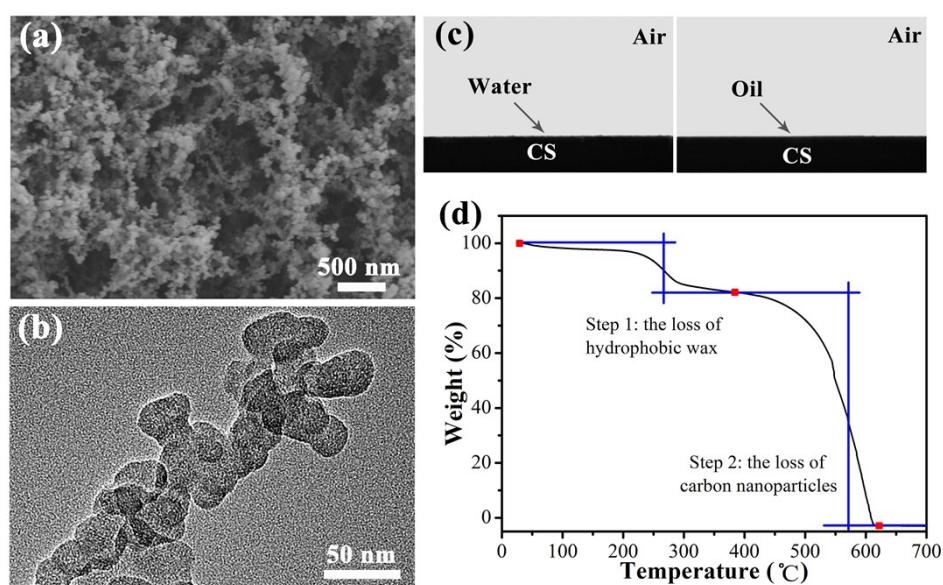


Fig. S1 (a) The FE-SEM image of CS in high magnifications; (b) the TEM image of the CS nanoparticles; (c) wetting behavior of CS in air. (d) TG curves of CS at a heating rate of $10\text{ }^{\circ}\text{C min}^{-1}$ in air flow.

The candle soot (CS) is very easy to collect just with a few seconds and constituted of regular carbon nanoparticles (20-50 nm).^[1] Fig.S1a and b reveals that the soot consists of carbon particles with a typical diameter of 30 to 40 nm, forming a loose, fractal-like network. The CS nanoparticles collected at center of flame shows a property of superhydrophobicity (the contact angle is as high as 154°) and a typical sp^2 carbon character^[2]. After calcination at $450\text{ }^{\circ}\text{C}$, the CS nanoparticles show superamphiphilicity in air, which is ascribed to the removal of the hydrophobic wax materials coated on the CS surface (Fig. S1c and d).^[2]

3. Preparation of CSM and CSP

Table S1 Dosage of reagent for fabricating CSM and CSP

	Mass of CS (g)	Volume of dispersion (mL)	Mass of agglomerant (g)	Drying process
CSM	0.04	Acetone, 30	PU, 0.024	70 °C, 2 h
CSP	0.05	Water, 40	SA, 0.184	40 °C, 4 h

4. Wettability of CSM

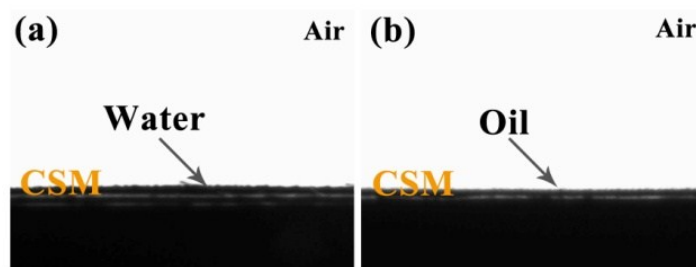


Fig. S2 (a) Wetting behavior of CSM toward water in air; (b) Wetting behavior of CSM toward oil in air. The oil droplet of kerosene was selected as the detecting probe.

5. Dynamic adhesion measurements

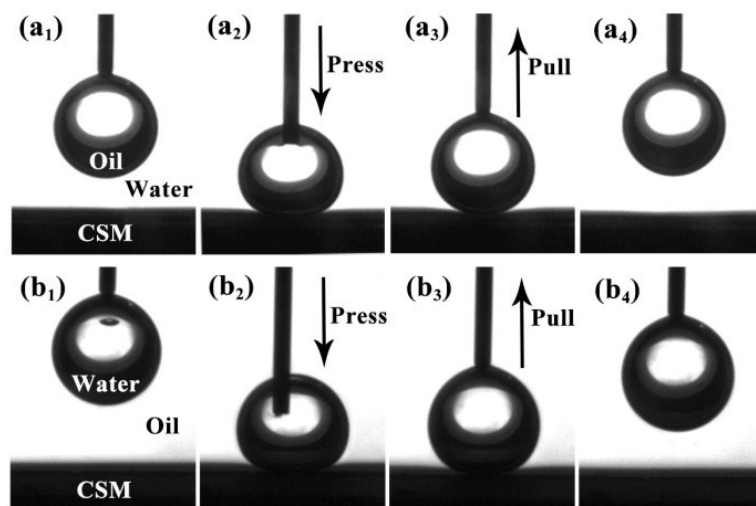


Fig. S3 dynamic adhesion measurements of (a) an oils droplet (chloroform) in water and (b) a water droplet in oil (kerosene). The volumes of oil and water droplet were 5 μL .

6. The wettability of the original stainless steel mesh

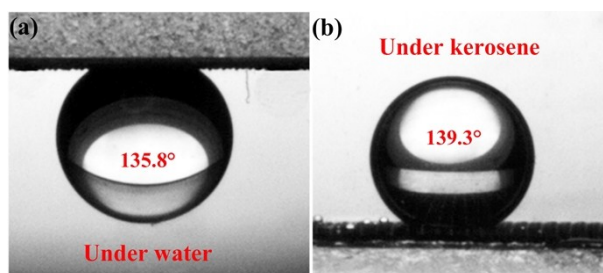


Fig. S4 The wettability of the original stainless steel mesh: (a) Under water; (b) Under oil.

As shown in Fig. S4, the original stainless steel mesh exhibited underwater oleophobicity with oil contact angle 135.8° and underoil hydrophobicity with water contact angle 139.3° . However, the original stainless steel mesh showed a high surface adhesion whether submerged in water or oil with the sliding angles larger than 25° .

7. Oil/water separation of the original stainless steel mesh

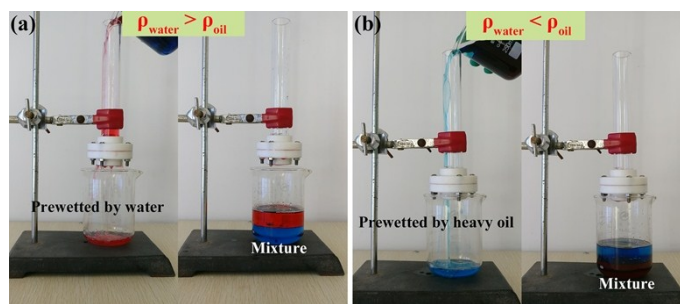


Fig. S5. Oil/water separation of the original stainless steel mesh.

When prewetted by water, the original stainless steel mesh could not remove water from the oil/water mixture (Fig. S5a). When prewetted by heavy oil, the original stainless steel mesh also could not separate heavy oil/water mixture.

8. The measurement of environmental stability

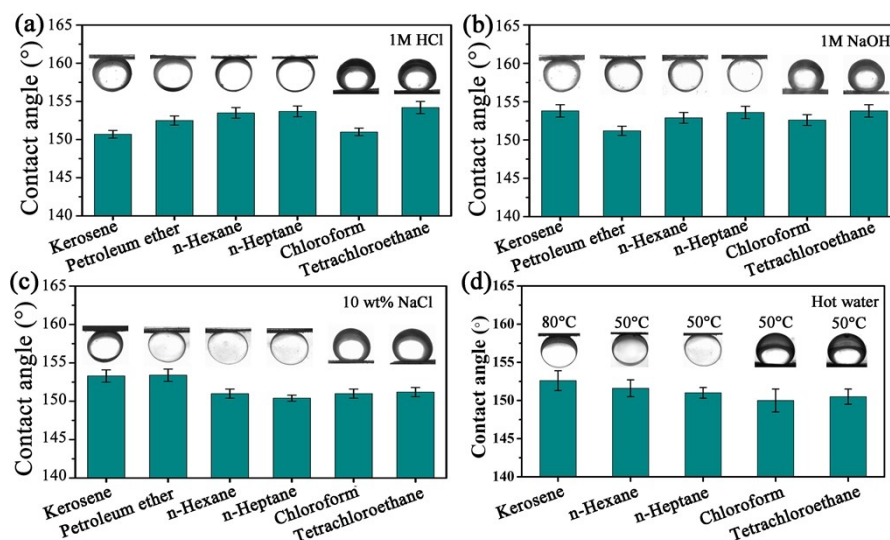


Fig. S6 The contact angles of oils under different corrosive and active solutions: (a) 1 M HCl, (b) 1 M NaOH, (c) 10 wt% NaCl solutions and (d) hot water

The CSM also showed stable underwater superoleophobicity towards many corrosive and active solutions (1 M HCl, 1 M NaOH, 10 wt% NaCl solutions and hot water), which was measured by immersing the coated mesh into corresponding solutions. As shown in Fig. S6, oil contact angles were all larger than 150°. The results show that CSM was chemically resistant to the extreme environment conditions.

9. The mechanical strength and abrasion resistance of the CMS

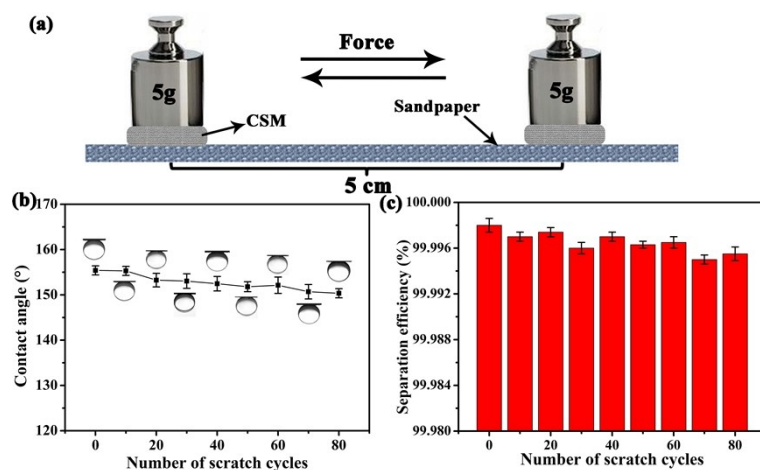


Fig. S7 (a) Schematic illustration of the scratch test. (b) The oil contact angle underwater versus the number of scratch cycles. (c) The separation efficiency of the CSM versus the number of scratch cycles.

As shown in Fig. S7a, the scratch test was carried out using 800 mesh SiC

sandpaper as an abrasion surface with the CSM facing the abrasion material. Simultaneously, the CSM was subjected to a 5 g weight and was dragged forward and backward with a speed and abrasion length of about 2 cm s^{-1} and 5 cm, respectively. Fig. S7b displayed the change in the oil contact angle as a function of scratch cycles. The results show that the oil contact angle underwater was still close to 150° after 80 scratch cycles. In addition, the separation efficiency remained above 99.99 % after 80 scratch cycles taking the kerosene/water mixture as an example. These results display that the CSM has good mechanical abrasion resistance.

10. The stability test of the CSP membrane

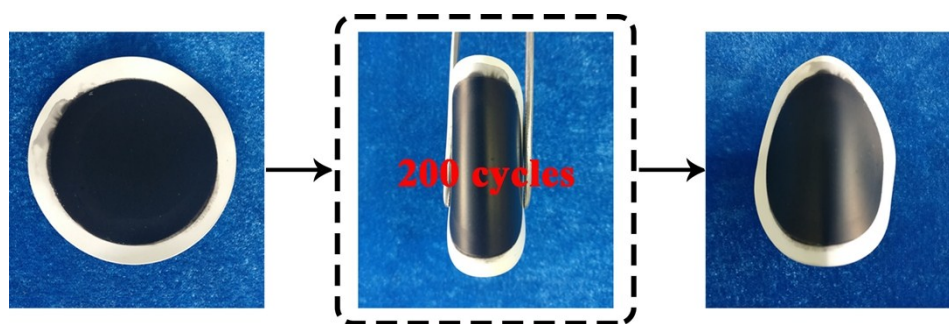


Fig. S8 Optical images of the CSP membranes before and after bending over 200 times.

To show the stability of the CSP membrane, the membrane was rolled up and released over 200 times. As shown in Fig. S8, there are no any cracks after bending cycles, indicating the excellent binding force between CS and PVDF substrate.

11. The wettability of the original PVDF

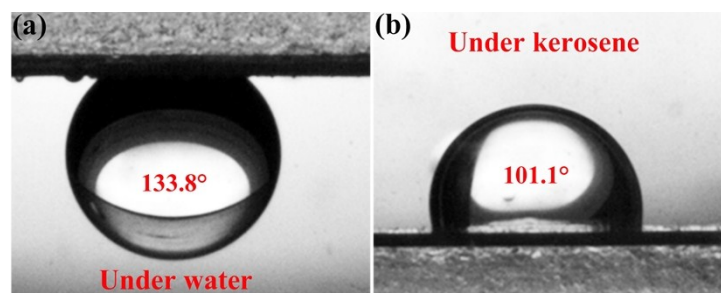


Fig. S9 The wettability of the original PVDF membrane: (a) Under water; (b) Under oil.

12. Water-in-oil and oil-in-water emulsions separation

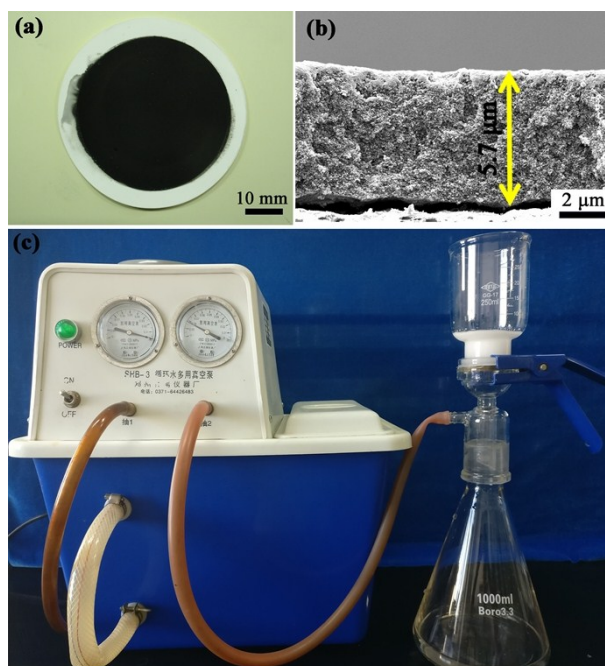


Fig. S10 (a) the CSP fabricated by leaching; (b) The FE-SEM images of CSP thickness; (d) The device for emulsion separation connected with a vacuum pump.

13. Stability tests of the emulsions and separation result of different membrane

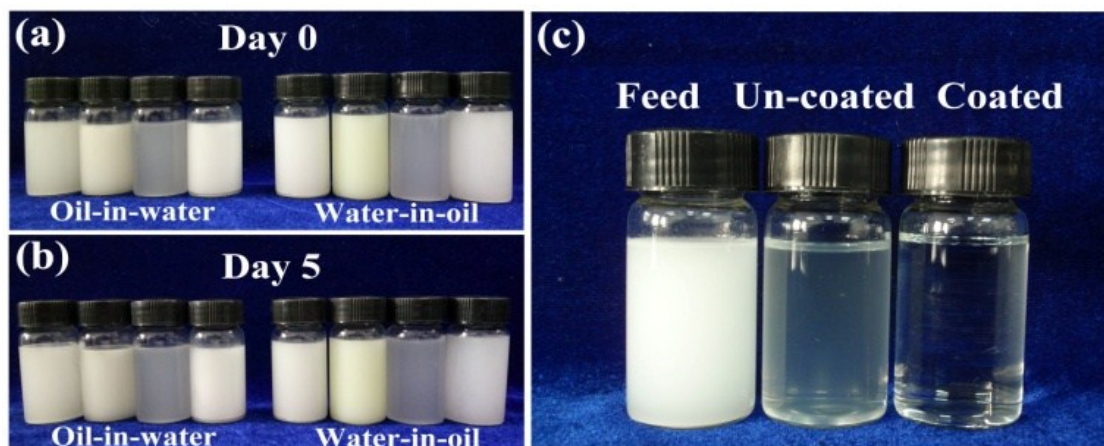


Fig. S11 (a, b) Stability tests of the various types of emulsions, after 5 days, the emulsions are still stable without demulsification. (c) Kerosene-in-water emulsion separation result of the original PDVB membrane (the middle vial) and the CSP (the right vial). The original PDVB membrane was not able to separate emulsion.

14. Optical microscope images and photographs of the demulsification and separation results for various types of oil-in-water emulsions

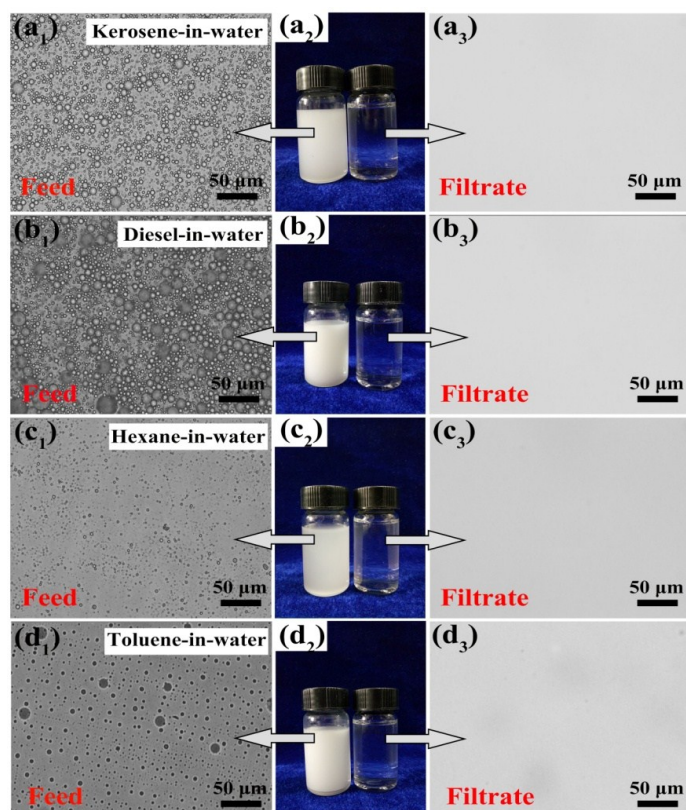


Fig. S12 Optical microscope images and photographs of the demulsification and separation results for various types of oil-in-water emulsions: (a) kerosene-in-water emulsion, (b) diesel-in-water emulsion, (c) hexane-in-water emulsions and (d) toluene-in-water emulsions. After separation, all the emulsions become transparent and no water droplets can be observed in the filtrates.

15. Optical microscope images and photographs of the demulsification and separation results for various types of water-in-oil emulsions

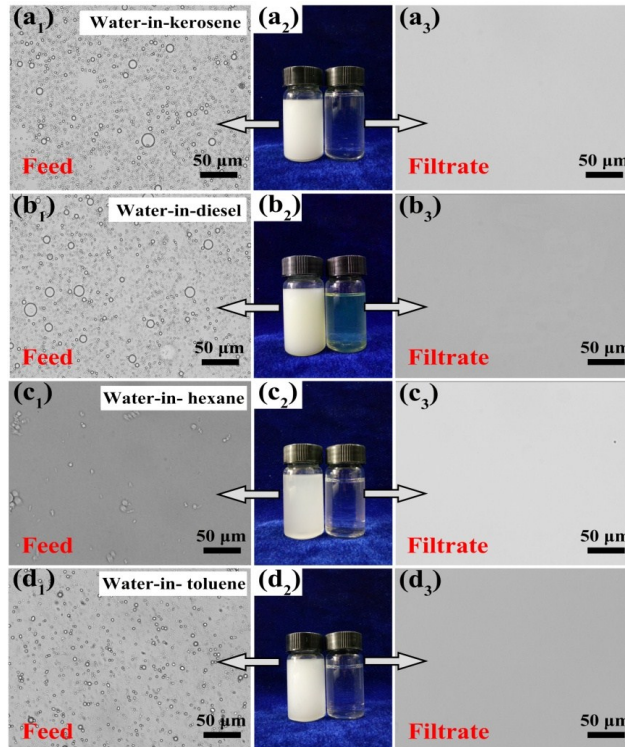


Fig. S13 Optical Microscope images and photographs of the demulsification and separation results for various types of water-in-oil emulsions: (a) water-in-kerosene emulsion (b) water-in-diesel emulsion and (c) water-in-hexane emulsions. After separation, all the emulsions become transparent and no water droplets can be observed in the filtrates.

16. Droplet size measurements of different stabilized emulsions for various types of emulsions

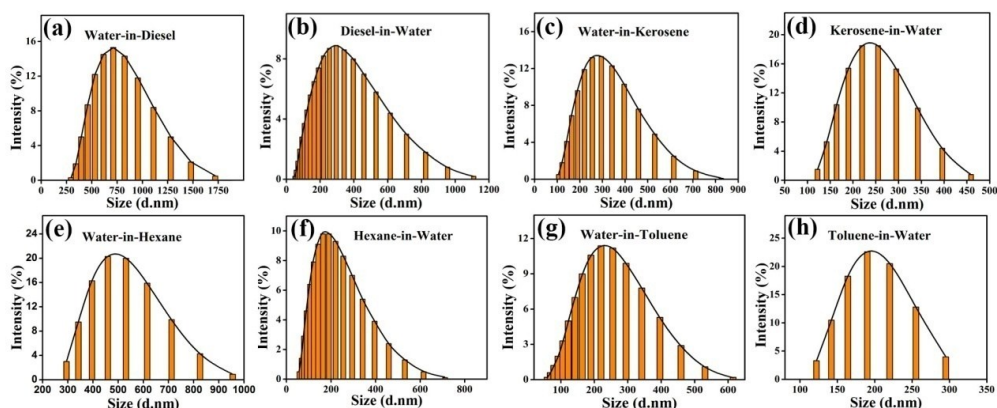


Fig. S14 Droplet size measurements of different stabilized emulsions for (a) water-in-diesel emulsion, (b) diesel-in-water emulsion, (c) water-in-kerosene emulsion, (d) kerosene-in-water emulsion, (e) water-in-hexane emulsion, (f) hexane-in-water

emulsion, (g) water-in-toluene emulsion and (h) toluene-in-water emulsion. For oil-in-water emulsion, most of the droplet sizes were less than 450 nm, while for water-in-oil, the droplet is a little bit larger.

17. Droplet size measurements of different filtrate after separation for various types of emulsions

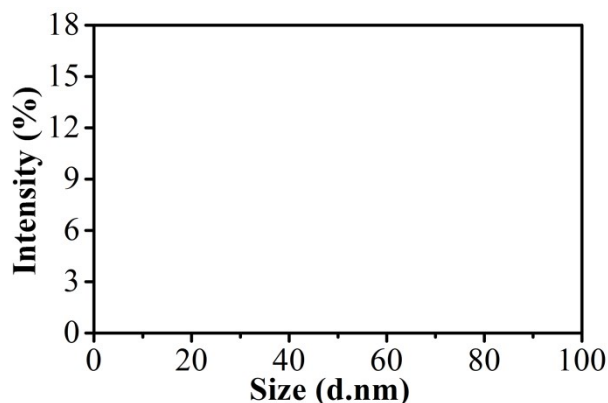


Fig. S15 Droplet size measurements of different filtrate for various types of emulsions including water-in-diesel emulsion, diesel-in-water emulsion, water-in-kerosene emulsion, kerosene-in-water emulsion, water-in-hexane emulsion, hexane-in-water emulsion, water-in-toluene emulsion and toluene-in-water emulsion.

18. Reference

- [1] X. Deng, L. Mammen, H. J. Butt, D. Vollmer, *Science* **2012**, 335, 67-70.
- [2] B. Zhang, D. Wang, B. Yu, F. Zhou, W. Liu, *RSC Adv.* **2014**, 4, 2586-2589.